NATIONAL ADVISORY COMMITTEE
FOR AERONAUTICS

TECHNICAL NOTE 4330

FLOW INDUCED BY A ROTOR IN POWER-ON VERTICAL DESCENT

By Walter Castles, Jr.

Georgia Institute of Technology

Washington

July 1958

.S

NATIONAL ADVISORY COMMITTEE FOR AERONAUTICS

TECHNICAL NOTE 4330

FLOW INDUCED BY A ROTOR IN POWER-ON VERTICAL DESCENT

By Walter Castles, Jr.

SUMMARY

Approximate equations are derived for the induced power required and blade loading of a lifting rotor operating in the power-on vertical-descent range. The approximate relations, which are based upon certain assumptions as to the nature of the flow pattern, yield, for the induced power variation, results which are in general agreement with the available experimental data.

INTRODUCTION

The induced power required in power-on vertical descent as predicted by elementary vortex theory or momentum theory based upon the assumption that a normal columnar wake extends a large distance below the rotor does not agree with the available experimental results as is seen from figure 1 (reproduced from ref. 1). Furthermore, the observed flow patterns about a rotor operating in power-on vertical descent are of a "vortex-ring" or recirculatory type for which it is necessary to consider the effects of viscosity and the resultant turbulent mixing in order to explain the existence of a steady thrust force.

Although the power-on vertical-descent flight range has been of little practical interest in the past on account of the operational limitations on single-engine helicopters, this flight range may be of considerable interest in the future if vertical-landing approaches are required at certain locations for multiengine helicopters or vertical-take-off-and-landing aircraft. A better understanding of the mechanics of the axially symmetric flows that occur in vertical descent may also be of value in that it may furnish some insight for the more complicated flow patterns that occur in inclined descent.

The present report is an attempt to express the relations between the rotor thrust loadings and induced velocity distributions for the vortex-ring or recirculatory flow patterns that exist in power-on vertical descent in a simple approximate manner that is suitable for engineering computations.

SYMBOLS

a slope of blade-element lift curve

b number of blades in rotor

c blade chord at radius r

c_{d_o} local blade profile drag coefficient at radius r

c_l blade-element lift coefficient

k slope of a linear variation of rotor disk loading along rotor
            radius

M' mass flow through rotor

P_c climb power, rate of change of potential energy

P_i induced power required

p static pressure

p_o atmospheric pressure

Q rotor torque

R rotor radius

r radius of point on rotor

T rotor thrust

V free-stream velocity or rate of descent

V_i local axial induced velocity at radius r

$V_o = \sqrt{w/2\rho}$

V_w axial velocity at end of wake core

v axial induced velocity at rotor for case of uniform disk
             loading

v_o axial induced velocity at hovering for hypothetical rotor

         with uniform disk loading, $\sqrt{\dfrac{T}{2\rho\pi R^2}}$

w disk loading at radius r

x nondimensional radius, r/R

Z distance below rotor

θ blade angle at radius r

ρ mass density of air

Ω angular velocity of rotor blades

ANALYSIS

Uniform Disk Loading

Consider the wake of an idealized lifting rotor hovering in a
viscous fluid as sketched in figure 2. Let the radial distribution of
loading be such as to impart a uniform increase in total pressure to
the fluid passing through the rotor. In analogy with the case of the
flow of a uniform, stationary, free jet as given in reference 2, there
will be a central region of the wake located below the cross section
of minimum radius AA', denoted in figure 2 by the region between the
axis and surface AB, within which the turbulent mixing has not pene-
trated and the flow will be essentially that of a nonviscous fluid
having a uniform axial velocity.

The mixing region between the sections AB and AC in figure 2 has
slightly divergent streamlines and an axial velocity distribution such
that the velocity decreases with radius from the wake center line and
with distance from the rotor.

In the case of the stationary free jet, it is remarked in ref-
erence 2 that experimental measurements show the static pressure to be
practically constant in the mixing zone and only very slightly above

atmospheric static pressure by the amount of the velocity head of the
radial velocity at the outer turbulent mixing boundary AC. It might
reasonably be supposed that a very similar situation exists with respect
to the uniformity of the static pressure in the mixing region at the
boundary of a rotor wake for the portion below the cross section of
minimum wake radius AA'.

It is to be noted that there is some surface, denoted by line AD
in figure 2, along which the axial velocity will be constant and some
small part, say equal to V, of the axial velocity at the rotor disk.
The radial components of velocity along such a surface of constant
axial velocity will be small compared with the axial velocity compo-
nents and will be directed outward.

Consider now the effect of imposing some small descent velocity,
say equal to the previously chosen value V, on the hovering flow pat-
tern of figure 2. Within the core of the wake previously enclosed by
the surface AB the principal effect will be similar to that obtained
by superposition of the velocity V; that is, there will be a decrease
in the axial velocities and little change in the radial velocities
somewhat as shown in figure 2. It would appear that the rate of
decrease of velocity along a streamline through the turbulent mixing
region between surfaces AB and AD will now be greater on account of
the path length being shorter, and the previous surface AD, somewhat
altered in position, will now constitute a surface of zero axial veloc-
ity as shown in figure 3. It would consequently follow that, except
for the effect of the very small radial velocity components, surface AD
now constitutes a surface of constant pressure similar to the surface AC
which existed in the hovering flow and along which, for the case of the
analogous free jet, the static pressure is practically constant. Since
surface AD in figure 3 contains the free-stream stagnation point D
where the static pressure is very nearly equal to the free-stream total
head, it might reasonably be supposed that the static pressure in the
turbulent mixing region between surfaces AB and AD in figure 3 is
approximately this same value.

As a check on the above hypothesis, static-pressure surveys were
made through the turbulent mixing region upstream of a 12-inch fan oper-
ating in the vertical-descent condition in the center of the 4-foot-square
free jet at the exit of the Georgia Institute of Technology low-
turbulence wind tunnel. The surveys, at three different radii and
free-jet velocities along lines parallel to the free-jet and fan axes,
were taken with a small pitot tube first directed toward the free
stream and then toward the fan. The results of the static-pressure
surveys are given in table I and are shown in figure 4. The test free-
jet velocities were limited to the speed range given in table I by
the reversal of rotation of the fan at higher velocities and the extreme

distortion of the free-jet boundaries at lower jet velocities. The lower velocity test conditions gave static-pressure peaks in the turbulent mixing region which were below the free-stream total head as would be expected from a consideration of the lack of constraint on the free-jet boundaries.

It can be seen from figure 4 that, within the accuracy of the present small-scale measurements, the static pressure in the turbulent mixing region at the end of the primary wake extending below a rotor operating at small rates of power-on vertical descent is of the order of the free-stream total head.

In figure 3 it is seen that, although there will be a certain amount of mixing over the whole of the local flow pattern, the greater part of the loss in total head in a fluid circuit must occur in the region ABDA which is the only region where there is a large velocity gradient. For steady-state conditions to exist, the loss in total head around a fluid circuit must be equal to the change in total head across the rotor or very nearly equal to the rotor disk loading for the idealized rotor under consideration. Similarly, it can be seen from figure 3 that the total head loss along a streamline within the core of the wake and extending from the rotor to section AB should be very small on account of the nearly uniform velocity distributions and consequent absence of turbulent mixing across these wake cross sections.

Consider now the effect of the small rate of vertical descent V on the outer boundary of the turbulent mixing region, represented by section AC in figure 2 for the case of hovering. For the descent case the outer turbulent-mixing-zone boundary AC in figure 2 will be folded back on itself, shrink to a line coinciding with the edge of the rotor, and be replaced by some section indicated by DE in figure 3. The momentum loss of the free-stream flow and the vorticity shed by the rotor will be confined within this outer wake boundary DE which, at large distances above the rotor, might be expected to have a diameter very nearly proportional to the cube root of the distance from the rotor in analogy with the wake at large distances behind any three-dimensional body exerting a drag force. There will be some dividing streamline, represented schematically by DF in figure 3, outside which the retarded free-stream flow within the outer wake boundary will continue to flow downstream and within which the fluid will recirculate through the rotor. For small rates of descent the upper stagnation point F will be a considerable distance above the rotor in a region of very low velocity flow and nearly atmospheric static pressure p_o. The total head along the axial entering streamline is thus of the order p_o. The total head loss in a circuit, which is the same for all the reentrant streamlines since it must be equal to the assumed uniform

disk loading for steady-state flow, is thus very nearly equal to the total head at the end of the wake core at section AB less the total head on an entering streamline, a value of the order of the ambient atmospheric pressure p_0.

Let the velocity at section AB where the static pressure is very nearly equal to the free-stream total head be denoted by V_w. Then the disk loading $T/\pi R^2$ is about equal to the total head at section AB minus the entering total head p_0. Thus

$$\frac{T}{\pi R^2} \approx \frac{1}{2}\rho V_w{}^2 + \frac{1}{2}\rho V^2 \tag{1}$$

or

$$V_w \approx \sqrt{\frac{2T}{\rho \pi R^2} - V^2} \tag{2}$$

It is to be noted that for the greater part of the energy loss in a circuit to occur in the high shear region between the section AB, where the total head is about $p_0 + \frac{1}{2}\rho\left(V_w{}^2 + V^2\right)$, and section AD, where the total head is about $p_0 + \frac{1}{2}\rho V^2$ plus some small radial velocity head, it is necessary that

$$V_w \gtrsim V \tag{3}$$

or from equation (2)

$$V \lesssim \sqrt{\frac{T}{\rho \pi R^2}} \tag{4}$$

The requirement that the downward-directed wake core velocity V_w at section AB in figure 3 be at least equal in order of magnitude to the free-stream velocity V can perhaps be seen more clearly from the

standpoint of vortex theory. The rate of transport of vorticity downward across some horizontal plane, say YY in figure 3, between sections AB and AD must be at least equal to the subsequent rate of transport of the same vorticity upward across YY between sections AD and DE for the presently assumed steady-state viscous flow. If the respective layers of vorticity are considered to compose diffuse vortex sheets, the vertical rates of transport of vorticity are equal to one-half the square of the respective vertical components of sheet strength or difference in vertical component of velocity across the sheets since the axial velocity component on the dividing section AD is zero by definition. If, as a first approximation, the effects of radial induced velocity components are neglected, the vertical velocity difference across the outer wake vortex sheet between sections AD and DE is equal to the free-stream velocity V, and thus the vertical velocity difference V_w across the inner wake sheet between sections AB and AD must be, to the same order of approximation, at least as great as V.

Another equation relating the thrust T and the wake core velocity V_w can be obtained from a consideration of the momentum exchange. Since linear momentum is preserved in the turbulent mixing process and the fluid recirculates, the rotor thrust can be no less than the rate of transport of axial momentum across section AB where the velocity is V_w and the total head is above the free-stream value. Let v be the mean axial component of induced velocity at the rotor. Then the mean resultant axial velocity at the rotor is v - V and the mass flow M' through the rotor is

$$M' = \rho \pi R^2 (v - V) \tag{5}$$

Thus the rate of change of axial momentum is

$$T = \rho \pi R^2 (v - V) V_w \tag{6}$$

Substituting the value of V_w from equation (2) in equation (6) and solving for the thrust, using the positive sign on the radical since the thrust does not vanish for hovering, give

$$T = \rho \pi R^2 (v - V) \left[(v - V) + \sqrt{(v - V)^2 - V^2} \right] \tag{7}$$

Solving equation (7) for the induced velocity v gives

$$v = V + \frac{v_o{}^2}{\sqrt{v_o{}^2 - \left(\frac{V}{2}\right)^2}} \qquad\qquad (8)$$

where

$$v_o = \sqrt{\frac{T}{2\rho\pi R^2}}$$

or in nondimensional form

$$\frac{v}{v_o} = \frac{V}{v_o} + \frac{1}{\sqrt{1 - \frac{1}{4}\left(\frac{V}{v_o}\right)^2}} \qquad\qquad (9)$$

It follows from equation (4) that the flight range for which equations (7), (8), and (9) are useful is

$$0 \lesseqgtr \frac{V}{v_o} \lesseqgtr \sqrt{2} \qquad\qquad (10)$$

Values of the nondimensional induced velocity v/v_o and the nondimensional rate of descent V/v_o are given in table II and shown in figure 5 along with the experimental curve for the values obtained in reference 1 for a model rotor with 12° blade twist and thus nearly uniform loading over the outer blade sections.

It is to be noted that for the rotor with uniform disk loading the relation

$$\frac{Tv}{Tv_o} = \frac{P_1}{Tv_o} = \frac{v}{v_o} \qquad\qquad (11)$$

$\Big($where P_i is the induced power required$\Big)$ holds so that figure 5 also gives the induced power ratios as indicated.

Triangular Distribution of Disk Loading Along Rotor Radius

The problem of finding the radial distribution of load, induced velocity, and thus the induced power required for a rotor with given blade geometry operating at a given rate of power-on descent by the method to be derived in the subsequent section involves the solution of a fourth-degree equation for the tangent of the inflow angle at the blade elements. Consequently the analysis of the present section will be restricted to a solution for the induced power required for a rotor with a given triangular distribution of disk loading along the rotor radius. This load distribution corresponds closely to that of a lifting rotor having blades with zero or small twist and it thus appears that, whereas the case of uniform loading is purely hypothetical, the case of triangular loading may be of considerable interest for purposes of performance estimation.

Let

$$w = k\left(\frac{T}{\pi R^2}\right)x \tag{12}$$

be the local disk loading at nondimensional radius x. Then

$$T = 2\pi k\left(\frac{T}{\pi R^2}\right)R^2 \int_0^1 x^2 dx \tag{13}$$

Integrating, solving the result for the constant k, and substituting the value of k in equation (12) give

$$w = \frac{3}{2}\left(\frac{T}{\pi R^2}\right)x \tag{14}$$

Define

$$V_o = \sqrt{\frac{w}{2\rho}} \tag{15}$$

in analogy with the value $v_o = \sqrt{\dfrac{T}{2\rho\pi R^2}}$ for the hypothetical case of

uniform loading. Then assuming that there is no turbulent mixing in the
primary wake core or, what amounts to the same thing, applying the
working hypothesis of the "independence of blade elements" over the
outer rotor annuli for which equation (9) applies gives

$$\frac{V_i}{V_o} = \frac{V}{V_o} + \frac{1}{\sqrt{1 - \frac{1}{4}\left(\frac{V}{V_o}\right)^2}} \tag{16}$$

where V_i is the local axial component of induced velocity at radius
r for the radii for which

$$0 \leqq \frac{V}{V_o} \leqq \sqrt{2} \tag{17}$$

Substituting the values of w and V_o from equations (14) and
(15) in equation (17) it is found that equation (16) is applicable for
the nondimensional radii

$$\frac{1}{3}\left(\frac{V}{V_o}\right)^2 \leqq x \leqq 1 \tag{18}$$

The nondimensional induced power $\left(P_i\right)_1 / Tv_o$ required for the
outer rotor annulus for which equation (18) holds is thus

$$\frac{\left(P_i\right)_1}{Tv_o} = \frac{2\pi R^2}{Tv_o} \int_{\frac{1}{3}\left(\frac{V}{V_o}\right)^2}^{1} wV_i x \, dx \tag{19}$$

or

$$\frac{\left(P_i\right)_1}{Tv_o} = 3 \int_{\frac{1}{3}\left(\frac{V}{V_o}\right)^2}^{1} \left[\frac{V}{V_o} + \frac{3x}{\sqrt{6x - \left(\frac{V}{V_o}\right)^2}}\right] x^2 dx \tag{20}$$

Integrating equation (20) gives

$$\frac{(P_i)_1}{Tv_o} = \left(\frac{V}{v_o}\right) - \frac{133}{1,890}\left(\frac{V}{v_o}\right)^7 +$$

$$\frac{\sqrt{6 - \left(\frac{V}{v_o}\right)^2}\left[1,080 - 216\left(\frac{V}{v_o}\right)^2 + 192\left(\frac{V}{v_o}\right)^4 + 4\left(\frac{V}{v_o}\right)^6\right]}{2,520} \quad (21)$$

It follows from setting $x = 1$ in equation (18) that the range of vertical descent for which equation (21) applies over some outer annulus of the rotor is

$$0 \leqq \frac{V}{v_o} \leqq \sqrt{3} \quad (22)$$

For the flight range specified by equation (22) the total pressure just beneath the rotor and inboard of nondimensional radius $x = \frac{1}{3}\left(\frac{V}{v_o}\right)^2$ is less than the static pressure in the turbulent mixing region at the lower end of the wake core. If the effects of turbulent mixing are neglected within the wake core, as was implied by the use of the independence of blade elements in deriving equation (21), this inner circle, for which $0 \leqq x \leqq \frac{1}{3}\left(\frac{V}{v_o}\right)^2$, constitutes a closed region as far as energy transfer from the rotor to the fluid is concerned. This is true because the fluid passing through these inner annuli would not have sufficient energy to penetrate the adverse pressure gradient above the turbulent mixing region; thus the total rotor torque due to lift for the sections of blades within the circle must be assumed to be zero. Using the hypothesis that the power input to the inner circle of the rotor for which $0 \leqq x \leqq \frac{1}{3}\left(\frac{V}{v_o}\right)^2$ is negligible, it follows that the induced power $(P_i)_2$ for this region is equal to the product of the thrust over the region and the rate of descent. Thus

$$\left(P_i\right)_2 = 2\pi V \int_0^{\frac{1}{3}\left(\frac{V}{V_0}\right)^2 R} wr \, dr \qquad (23)$$

Substituting the value of the disk loading w from equation (14) and dividing both sides by Tv_0 give the nondimensional induced power increment

$$\frac{\left(P_i\right)_2}{Tv_0} = 3\left(\frac{V}{V_0}\right) \int_0^{\frac{1}{3}\left(\frac{V}{V_0}\right)^2} x^2 dx = \frac{1}{27}\left(\frac{V}{V_0}\right)^7 \qquad (24)$$

The nondimensional induced power for the rotor with triangular loading operating in the power-on vertical-descent range is the sum of the parts given by equations (21) and (24). The computed values are given in table III. Figure 6 shows the comparison of the computed values with the experimental values given in reference 1 for a 6-foot-diameter constant-chord rotor with untwisted blades. The values obtained on a full-scale flight test of a rotor with untwisted blades as given in reference 3 are also shown. The flight-test results include the effects of fuselage drag which tend to make these experimental values too large at low descent velocities and probably too small at large descent velocities. The theoretical results of the present investigation are seen to be in satisfactory agreement with the experimental results.

Loading Over Outer Blade Elements of a Rotor

With Arbitrary Blade Geometry

From two-dimensional airfoil theory it follows that, for small inflow angles, the thrust dT on a rotor annulus of radius r and width dr is

$$dT = \frac{1}{2}\rho abc(\Omega r)^2 \left[\theta - \left(\frac{v_1 - V}{\Omega r}\right)\right] dr \qquad (25)$$

where

a   slope of blade-element lift curve

b   number of blades in rotor

c   local blade chord at radius r

Ω angular velocity of rotor

θ local blade angle at radius r

Writing equation (7) in differential form for the annulus,

$$dT = 2\rho\pi r\left(V_i - V\right)\left[\left(V_i - V\right) + \sqrt{\left(V_i - V\right)^2 - V^2}\right]dr \qquad (26)$$

for $V_i \gtreqless 2V$.

Equating the right sides of equations (25) and (26) gives the following equation:

$$\frac{abc}{4\pi r}\left[\theta - \left(\frac{V_i - V}{\Omega r}\right)\right] = \left(\frac{V_i - V}{\Omega r}\right)\left[\left(\frac{V_i - V}{\Omega r}\right) + \sqrt{\left(\frac{V_i - V}{\Omega r}\right)^2 - \left(\frac{V}{\Omega R}\right)^2}\right]$$
$$(27)$$

Equation (27) may be solved graphically or otherwise for the radial distribution of the induced velocity V_i and the inflow angle for the applicable radii for which $V_i \gtreqless 2V$. The thrust loading may then be computed from equation (25) and the torque loading dQ on the rotor annulus of width dr from the usual blade-element equation

$$dQ = dT\left(\frac{V_i - V}{\Omega r}\right) + \left(\frac{1}{2}\rho bc\Omega^2 r^3 c_{d_o}\right)dr \qquad (28)$$

where c_{d_o} is the profile drag coefficient for the blade element at radius r and lift coefficient

$$c_l = a\left[\theta - \left(\frac{V_i - \bar{V}}{\Omega r}\right)\right] \tag{29}$$

The simplest consistent assumption for the distribution of the inflow angle over the inner radii for which $V_i < 2V$ in equation (28) is that $V_i = V$ for this inboard region. However, such a zero value for the inflow angle really constitutes a weighted average for the induced torque rather than an actual distribution. Consequently, if this assumption is made, it would be necessary to assume also a reasonable blade-thrust distribution such as a parabolic variation from the calculated value at the limiting radius $x = \frac{1}{3}\left(\frac{V}{V_o}\right)^2$ to a zero value at the hub.

It appears that the above approximation should be adequate for small rates of vertical descent where the limiting radius is small and the thrust in question is an immaterial part of the total.

CONCLUDING REMARKS

The present analysis appears to yield results for the variation of induced power with rate of vertical power-on descent for a lifting rotor which are in satisfactory agreement with the available experimental data. It may thus be useful in performance estimation and in furnishing some insight into the mechanics of the vortex ring or recirculatory flows that occur in these flight conditions.

As there are no experimental blade-load or direct induced-velocity measurements available for comparison, some judgment should be exercised in the application of the theoretical blade-load equations given in the paper.

It might be pointed out that the present analysis gives no steady-state solution for the (hypothetical) rotor with uniform disk loading operating in the power-on descent range where the ratio of the free-stream velocity to the induced velocity in hovering is greater than the square root of 2. In the case of any actual lifting rotor the disk loading will go to zero at the hub and the radial distribution of disk loading will be dependent upon the rate of descent. Consequently, it might be expected that the range of stable operation for any actual rotor will be larger than that for the hypothetical case of uniform loading.

The question arises as to why an analysis of the present type should predict the ideal autorotation point or rate of descent at which the induced power required is equal to the rate of decrease of potential energy and the resultant mean normal component of velocity at the rotor is consequently zero. One explanation of this question might be as follows.

The idealized flow pattern or perfect-fluid flow patterns for a lifting rotor operating at the ideal autorotation point would have to be of the Kirchhoff or free-streamline type where the whole of the wake above the rotor and extending downstream to infinity constitutes a closed energy region. In the corresponding viscous-fluid flow pattern a closed energy region bounded by the turbulent mixing zone would also exist within which the flow could be considered to be of perfect-fluid type. However, in this case it would be a closed region bounded by the upper surface of the rotor and some surface of revolution extending a limited distance downstream.

The present analysis hypothecates the existence of such a closed energy region enveloping the inboard blade elements at some small rate of vertical descent and increasing in diameter with rate of descent until, at the ideal autorotation point, it includes the full rotor radius. The growth in diameter of the closed energy region with rate of descent would necessarily be determined by the external flow and consequently the ideal autorotation point would occur when the downflow through the outer rotor annulus vanishes. The prediction of the rate of descent at which the downflow through the outer blade elements disappears thus gives the rate of descent at the ideal autorotation point.

Georgia Institute of Technology,
    Atlanta, Ga., March 22, 1957.

REFERENCES

1. Castles, Walter, Jr., and Gray, Robin B.: Empirical Relation Between
     Induced Velocity, Thrust, and Rate of Descent of a Helicopter Rotor
     as Determined by Wind-Tunnel Tests on Four Model Rotors.   NACA
     TN 2474, 1951.

2. Prandtl, L.:   The Mechanics of Viscous Fluids.   Spread of Turbulence.
     Vol. III of Aerodynamic Theory, div. G., sec. 25, W. F. Durand,
     ed., Julius Springer (Berlin), 1935, pp. 162-178.

3. Stewart, W.:   Flight Testing of Helicopters.   Jour. R.A.S., vol. 52,
     no. 449, May 1948, pp. 261-292; discussion, pp. 293-304.

TABLE I

RESULTS OF STATIC MEASUREMENTS

(a) Run 1: Fan 5 diameters from free-jet exit; free-jet velocity,
17.5 feet per second; survey along a line 0.5R from axis.

$\dfrac{Z}{D}$	$\dfrac{p - p_o}{\frac{1}{2}\rho V^2}$	$\dfrac{Z}{D}$	$\dfrac{p - p_o}{\frac{1}{2}\rho V^2}$ (a)
0.96	0.83	0.42	0.25
1.17	1.00	.58	.33
1.33	.92	.75	.67
1.50	.83	.83	.75
1.67	.75	.92	.83
2.50	.25	1.00	.92
3.33	.08	1.08	1.00
		1.17	1.00
		1.33	.92

(b) Run 2: Fan 4 diameters from free-jet exit; free-jet velocity,
16.5 feet per second; survey along a line 0.6R from axis.

$\dfrac{Z}{D}$	$\dfrac{p - p_o}{\frac{1}{2}\rho V^2}$	$\dfrac{Z}{D}$	$\dfrac{p - p_1}{\frac{1}{2}\rho V^2}$ (a)
0.58	0.60	0.25	0.60
.83	.82	.46	.64
1.33	.97	1.00	.97
1.83	.67	1.50	.75
2.33	.40	2.00	.45
2.83	.25		
3.33	.12		

[a]Static pressure for pitot facing fan.

TABLE I.- Concluded

RESULTS OF STATIC MEASUREMENTS

(c) Run 3: Fan 5 diameters from free-jet exit; free-jet velocity,
      14.2 feet per second; survey along a line at 0.33R from axis.

$\frac{Z}{D}$	$\dfrac{p - p_o}{\frac{1}{2}\rho V^2}$	$\frac{Z}{D}$	$\dfrac{p - p_o}{\frac{1}{2}\rho V^2}$ (a)
1.13	0.75	0.58	0
1.25	.75	.83	0
1.33	.87	1.08	.25
1.42	1.00	1.17	.37
1.50	1.00	1.25	.75
1.67	1.00	1.33	.87
2.00	.75	1.42	.87
2.50	.50	1.50	.75
3.33	.12		

[a]Static pressure for pitot facing fan.

TABLE II

VALUES OF NONDIMENSIONAL INDUCED VELOCITY AND NONDIMENSIONAL RATE OF

DESCENT FOR IDEALIZED ROTOR WITH UNIFORM LOADING

V/v_o	v/v_o
0	1.000
.2	1.205
.4	1.420
.6	1.658
.8	1.892
1.0	2.155
1.2	2.450
1.4	2.801
$\sqrt{2}$	$2\sqrt{2}$

TABLE III

THEORETICAL VALUES OF NONDIMENSIONAL INDUCED POWER RATIO P_i/Tv_o AND

NONDIMENSIONAL RATE OF DESCENT V/v_o FOR ROTOR WITH TRIANGULAR

DISTRIBUTION OF DISK LOADING ALONG RADIUS

V/v_o	P_i/Tv_o
0	1.049
.2	1.238
.4	1.407
.6	1.568
.8	1.737
1.0	1.907
1.2	2.079
1.4	2.185
1.6	2.069
1.65	1.974
1.70	1.841
$\sqrt{3}$	$\sqrt{3}$
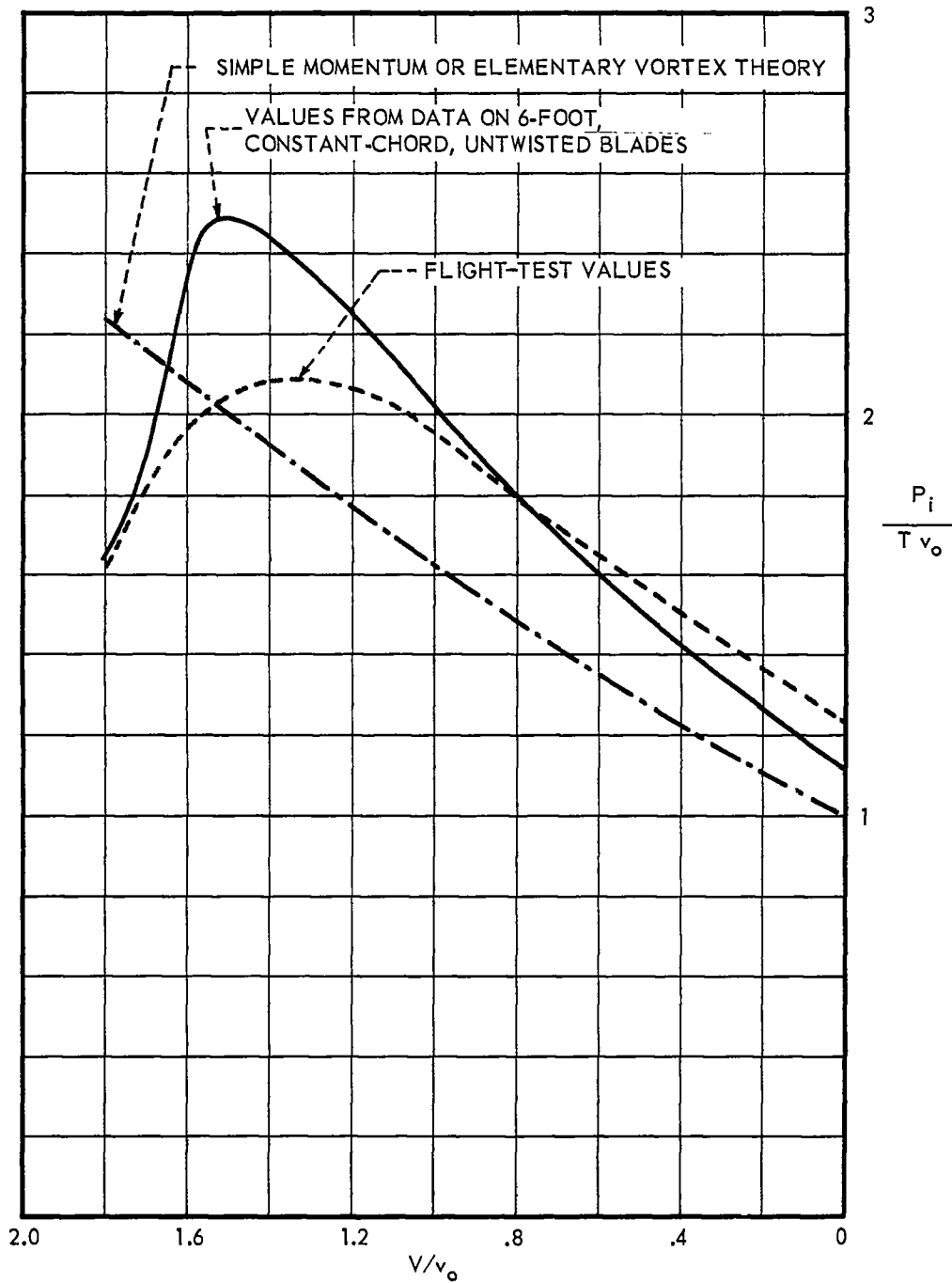
Figure 1.- Comparison of values of nondimensional induced power for
power-on vertical descent given by simple momentum theory or elementary vortex theory with experimental values.
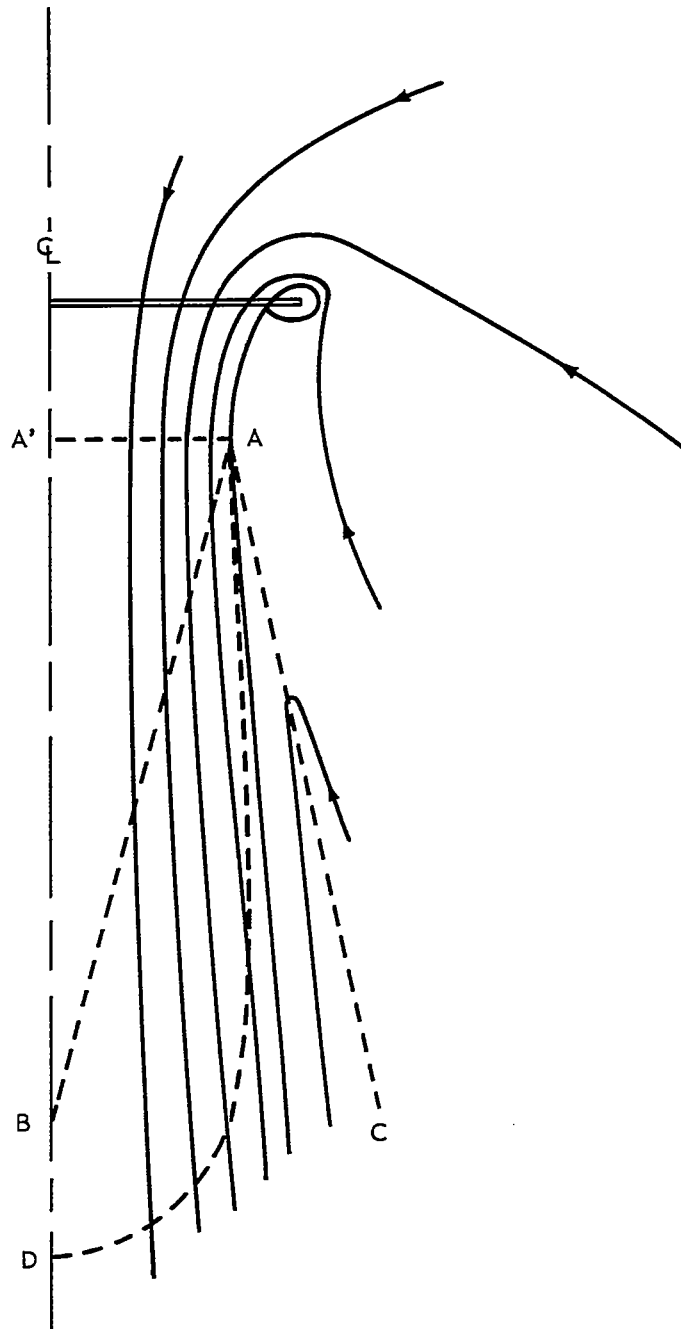
Figure 2.- Sketch of idealized hovering air-flow pattern. AA', minimum
wake radius; AB, outer boundary of region of no mixing; AC, outer
boundary of mixing region; AD, line of constant axial velocity in
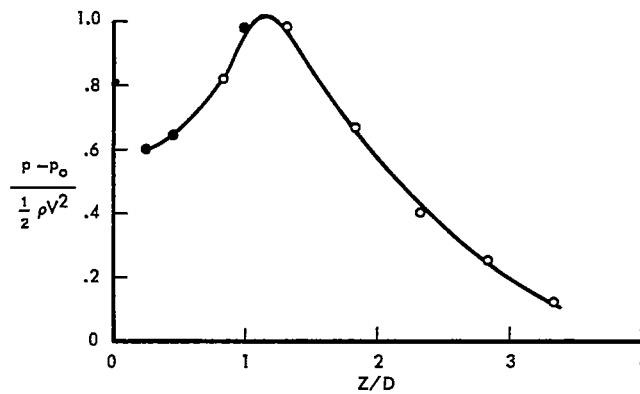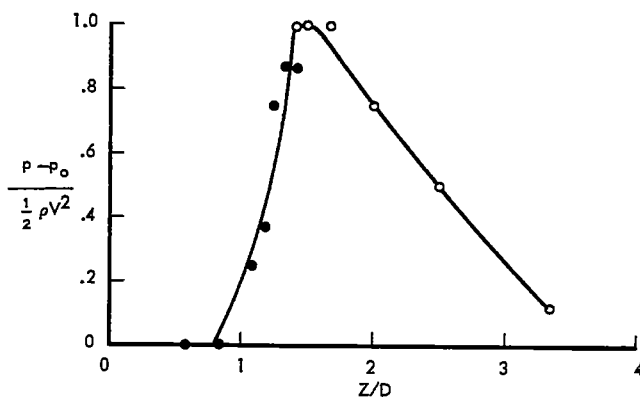mixing region.
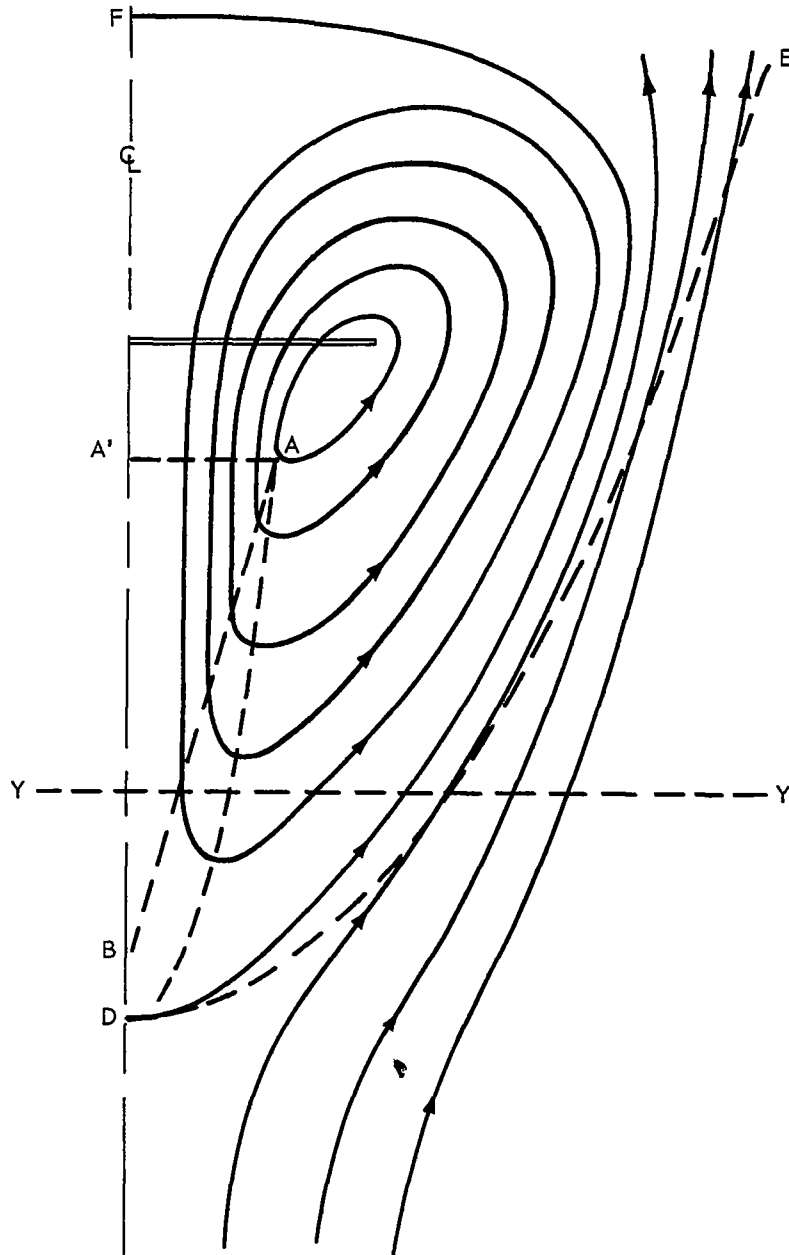
Figure 3.- Sketch of idealized air-flow pattern at small rate of verti-
cal descent for rotor with uniform loading. AA', minimum wake
radius; AD, line of zero axial velocity; DE, outer boundary of
mixing region; AB, outer boundary of region of no mixing; DF, stream-
line dividing recirculatory and downstream flow; F, point in region
of very low velocity and nearly static pressure; YY, horizontal
plane through rotor wake.
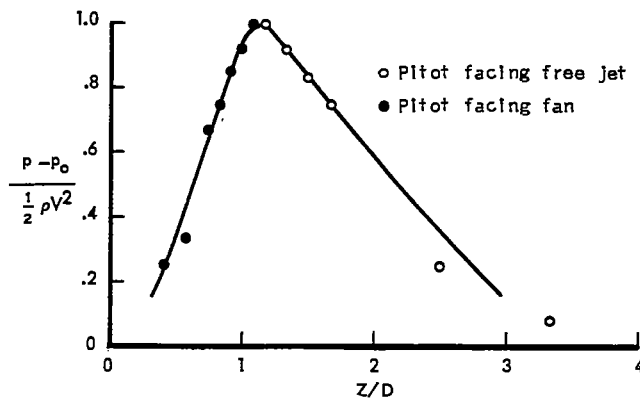
(a) Run 1: V = 17.5 feet per second; traverse at 0.50R.

(b) Run 2: V = 16.5 feet per second; traverse at 0.60R.

(c) Run 3: V = 14.2 feet per second; traverse at 0.33R.

Figure 4.- Variation of static pressure through turbulent mixing region.
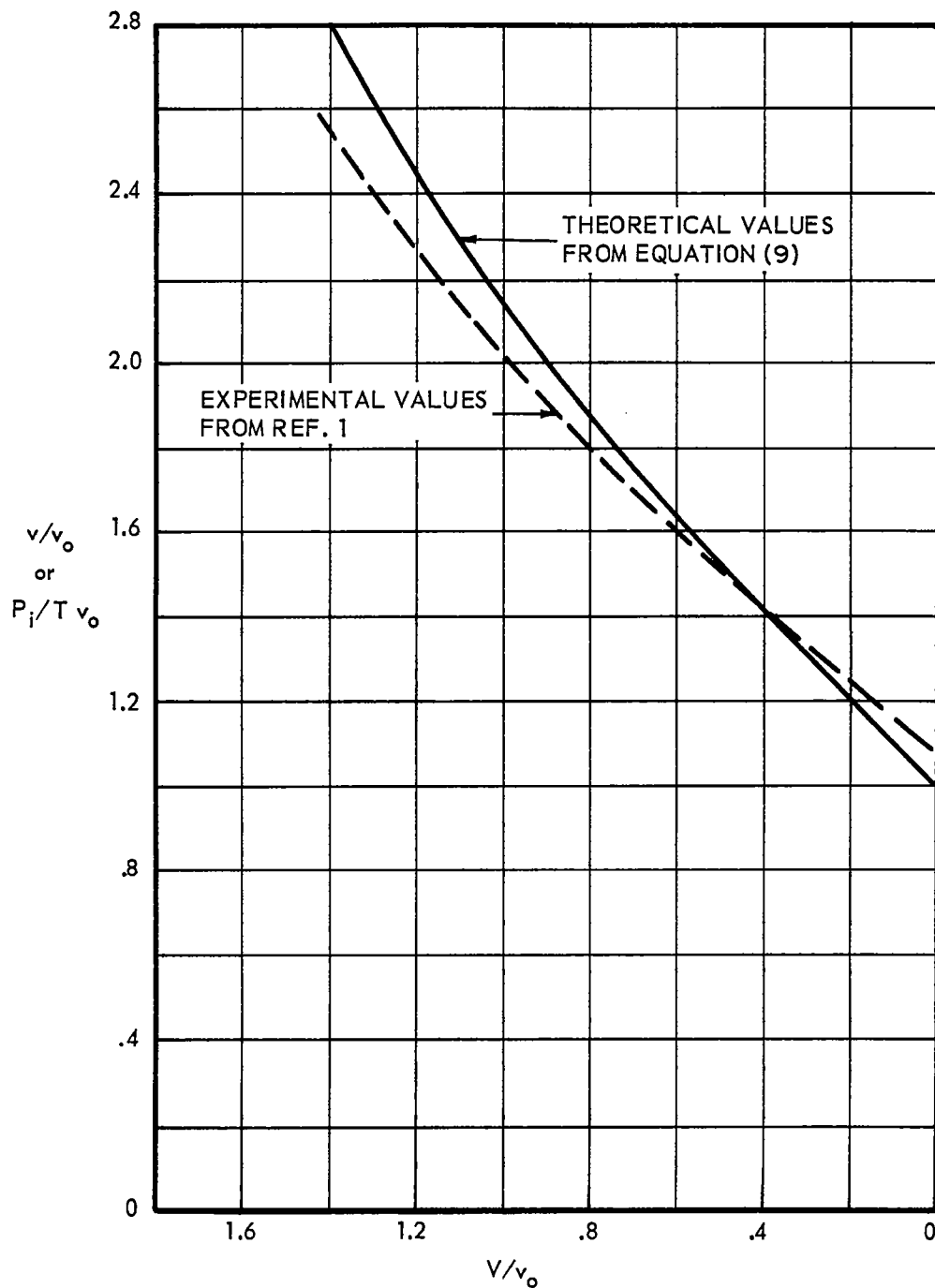
Figure 5.- Comparison of theoretical values of nondimensional induced
    velocity for uniform disk loading with experimental values for model
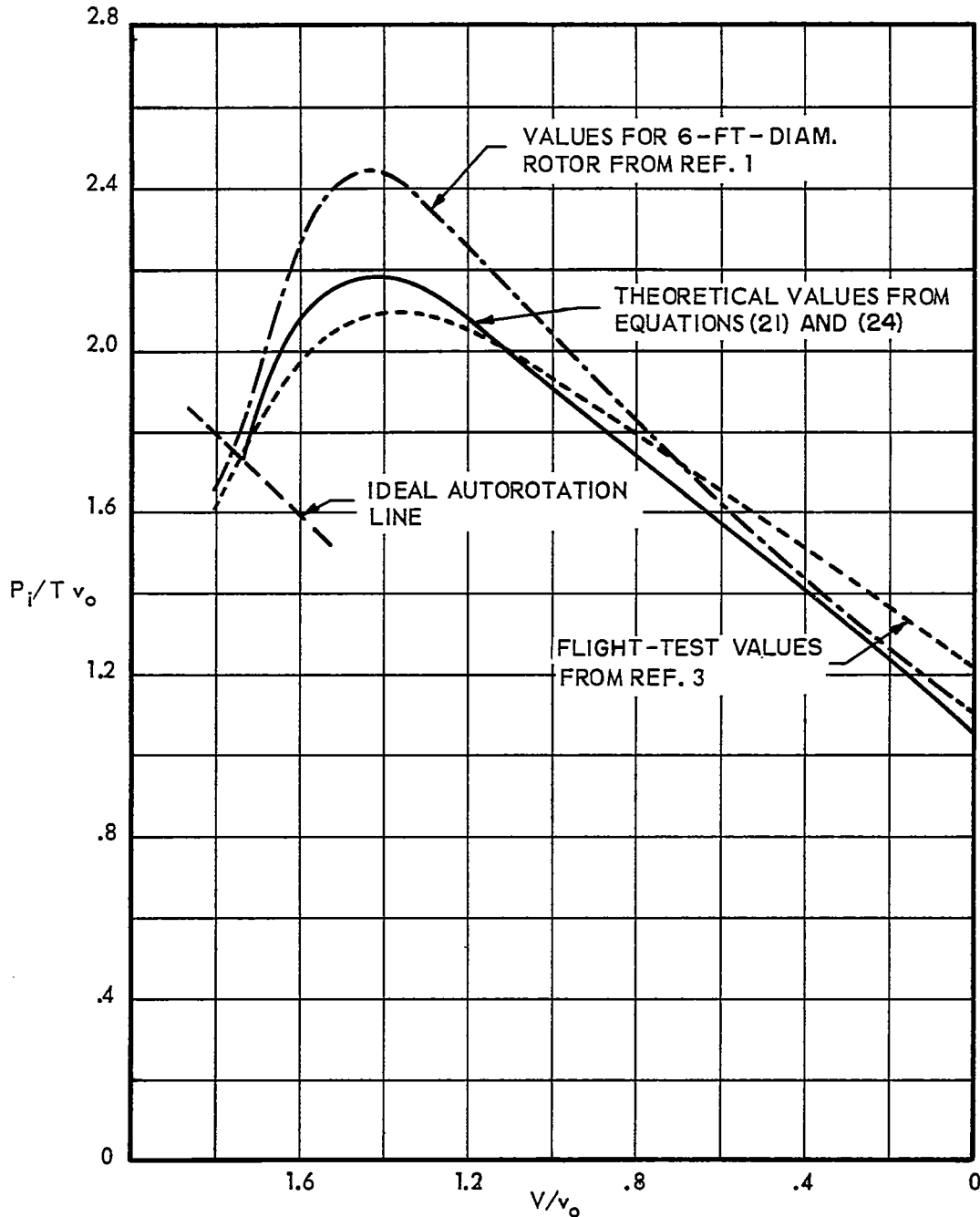   rotor with 12° blade twist.

Figure 6.- Comparison of theoretical induced power ratios plotted against nondimensional rates of vertical descent for rotor with triangular distribution of radial disk load with experimental values for rotors with untwisted blades.